Original Article
In vitro evaluation of rhBMP-2-induced expression of VEGF in human adipose-derived stromal cells

Yi Yang[1*], Gele Jin[1*], Xin Cao[2], Peng Wang[2], Xinming Yang[1], Jiang Wu[3]

[1]Orthopaedic Centre, The First Affiliated Hospital of Xinjiang Medical University, China; [2]Central Hospital of Shengli Oil Field, Dongying, China; [3]School of West China Basic Medicine and Forensic Medicine, Sichuan University, Chengdu 610041, China. *Equal contributors.

Abstract: Bone Morphogenetic Protein 2 (BMP-2) plays a key role in skeletal development, repair and regeneration. Our previous studies indicate that recombinant human BMP-2 (rhBMP-2) can stimulate osteogenic differentiation and promote angiogenesis through the up-regulation of Vascular Endothelial Growth Factor (VEGF), while the underlying mechanism of the BMP-2 effect on human cells is not well understood. To gain a better understanding of BMP-2-induced angiogenesis, we further characterized the effect of rhBMP-2 on VEGF expression in human adipose-derived stromal cells (hASCs) by RT-PCR and ELISA. VEGF expression was induced by rhBMP-2 in a dose- and time-dependent manner, with the highest induction observed using 100 ng/ml of rhBMP-2 at 18-24 h post stimulation. In addition, Western blot analyses revealed that the phosphorylation of p38 was closely related to the expression of VEGF, and blocking the p38MAPK pathway with the specific inhibitor sb203580 resulted in the decreased VEGF expression. Our data suggest that p38 activation may be required for rhBMP-2-induced VEGF expression and angiogenesis. Information derived from this study may shed light on understanding the effect of rhBMP-2 in the angiogenesis of hASCs, which is important for designing new strategies to increase the angiogenesis of tissue engineering bone.

Keywords: rhBMP-2, hASC, VEGF, angiogenesis, p38MAPK, tissue engineering bone

Introduction

Reconstruction of bone defects is an extremely challenging medical task. Bone tissue usually has the ability to repair itself, but when a defect reaches to a critical size, the repair attempt fails in most cases, resulting in the formation of pseudarthrosis, also called "non-union" of the fracture, and loss of function. Autograft is the most effective method for bone restoration, because it provides three essential elements: osteoconduction, osteoinduction and osteogenic cells. However, its source is limited and may cause complications at the donor sites, thus restricting its clinical applications [17, 24]. Allograft is believed to be osteoconductive; but it confers the risk of disease transmission and immune rejection [8]. Synthetic bone substitutes are commonly used to treat large bone defects; however, these therapies are associated with high rates of failure as a result of incomplete vascularization and bone remodel-

ing [15]. The technology of bone tissue engineering provides an advanced and promising therapeutic strategy for the repair of bone defects, especially the critical-sized bone defects resulting from trauma, surgical resection and congenital deformity corrections [4, 19]. Vascularization is the key challenge in tissue engineering [5]. The success of transplantation is dependent on adequate vascularization at the initial stage. In the absence of blood vessels, engineered tissue cannot be perfused with oxygen, nutrients and cells involved in the regenerative process. Current strategies for vascularization in tissue engineering are related to growth factor signaling, cell transplantation, bioactive smart matrix materials and directed fabrication [3, 20, 21, 29].

Bone Morphogenetic Proteins (BMPs) belong tothe Transforming Growth Factor-beta (TGF-β) superfamily and play key roles in the development of bone and cartilage across all species.

BMP-2 is involved in several processes during bone morphogenesis, ncluding bone remodeling, bone formation, chondrogenesis and mesenchymal cell infiltration and proliferation [23, 25]. Our previous studies showed that rhBMP-2 not only stimulated osteogenic differentiation, but also promoted angiogenesis through up-regulation of Vascular Endothelial Growth Factor (VEGF). Similar results were reported by others [13]. BMP-2 has promising prospect in bone repair because of these effects, while unbeneficial applications of rhBMP-2 may cause catastrophic complications [22]. Therefore, detailed biological characteristics of the BMP-2 effect on VEGF induction in human cells need to be documented.

It has been demonstrated that the Mitogen Activated Protein Kinase (MAPK) signal pathway plays important roles in cellular responses to hormones, cytokines, physical stress and other environmental stimuli [11]. MAPK family includes at least three distinctly regulated groups: extracellular signal-related kinases (ERK) 1/2, Jun amino-terminal kinases (JNK1/2/3), and p38 mitogen-activated protein kinase (p38 MAPK) [11]. Recent studies demonstrated that the p38MAPK pathway can be activated by BMP-2, which plays critical roles during BMP-2-induced cell migration, differentiation and mineralization [7, 27]. It has been shown that p38 is also involved in the regulation of VEGF expression. It has been demonstrated that the p38 MAPK pathway is essential for skeletogenesis and bone homeostasis in mice [10]. The p38 MAPK pathway has also been shown to be important for shear stress-induced angiogenesis and VEGF expression [9]. Based on these results, we speculate that the p38MAPK pathway may play a predominant role in rhBMP-2-induced VEGF expression and angiogenesis. In the present study, we studied the biological characteristics of BMP-2-induced VEGF expression inhuman adipose-derived stromal cells (hASCs) at both RNA and protein levels. In addition, the role of p38MAPK pathway in the regulation of VEGF expression was investigated.

Materials and methods

Isolation and culture of hASCs

Fresh human adipose tissues were obtained from three healthy patients (at an average age of 28 years) with informed consent, who re-ceived operations at the First Affiliated Hospital of Xinjiang Medical University. The research protocols were approved by the Research Ethical Committee of the Hospital. The cell isolation and culture were performed as previously described [2, 30]. Briefly, adipose tissues were washed extensively with sterile phosphate-buffered saline (PBS) for three times, and blood vessels and fibrous tissues were carefully removed. Subsequently, adipose tissues were digested with 0.075% collagenase type I (Sigma, USA) at 37°C for 60 min. Enzymatic activity was neutralized with low glucose Dulbecco's modified Eagle's medium (LG-DMEM, Gibco, USA) containing 10% fetal bovine serum (FBS, Gibco, USA), and the digested tissues were centrifuged at 1200 g for 10 min to obtain a high-density stromal vascular fraction (SVF). The tissue pellet was then treated with red blood cell lysing buffer (0.3 g/L ammonium chloride in 0.01 MT rise HCl buffer, pH 7.5, Sigma) for 5 min, centrifuged at 600 g for 10 min, and then filtered through a 100-mm nylon mesh to remove the undigested tissue. Cells were suspended in LG-DMEM medium containing 10% FBS, 100 mg/mL streptomycin and 100 U/mL penicillin, and plated at 4×10^4 cells/cm^2 in 100 mm culture dishes. After 48 hours, cells were washed with PBS to remove dead cells, and continued to culture in the same medium as above, which was renewed every three days. When reached 70-80% confluence, cells were passaged and hASCs at passage 3 were used in the current study.

Characterization of hASCs

hASCs were characterized by Fluorescence Activated Cell Sorter analysis(FACS) to detect cell surface antigens. For FACS, cells were incubated in Dulbecco's modified eagle's medium solutions containing antibodies at 4°C for 30 min and washed with PBS containing 2% (v/v) serum. The labeled cells were analyzed using a BD FACS Calibur system. To test the multi-differentiation capacity of hASCs, cells were got from patients who received liposuction and were cultured with either osteogenic- or adipo-genic- inducing media for 14 days. Alkaline phosphatase (ALP) stains were used to visualize osteogenesis according to the staining step on the instruction and Oil red O stains were used to visualize adipogenesis according to the staining step on the instruction [14].

Treatment of hASCs

hASCs were treated with rhBMP-2 (Peprotech, USA) at different concentrations at passage 3 when reached 70-80% confluence. Culture medium was removed and cells were washed twice with PBS. rhBMP-2 was added at 0 ng/ml, 50 ng/ml, 100 ng/ml, and 200 ng/ml to the fresh LG-DMEM containing 10% FBS, 100 mg/ml streptomycin and 100 U/ml penicillin. Cells were treated for various time points, and then collected for subsequent assays.

Pretreatment with p38 inhibitor sb203580

hASCs at passage 3 with 70-80% confluence were washed twice with PBS, and pre-treated with 0, 5, 15 µM of sb203580 (Invitrogen, USA) in LG-DMEM containing 10% FBS, 100 mg/ml streptomycin and 100 U/mL penicillin for 30 min. Cells were then treated with 100 ng/ml of rhBMP-2 for 24 h and harvested for subsequent analyses.

Reverse transcription PCR (RT-PCR) analyses

Total RNA was extracted from cells using a Trizol reagent (Invitrogen, USA) according to the single step acid-phenol guanidinium extraction method. 1 g of RNA was reversely transcribed for first strand cDNA synthesis using PrimeScript 1st Strand cDNA synthesis kit (Fermentas, Canada). The PCR amplification was performed in a Thermal Cyclerat 94°C for 5 min, 94°C for 30 s, 55°C for 30 s, 72°C for 30 s for 35 cycles, and then extended at 72°C for 7 min. The amplified products were subjected to electrophoresis and the results were analyzed by gel imaging and analysis system (Bio-Rad, USA). The GAPDH housekeeping gene was served as a control. The primers used are listed below.

VEGF-forward 5'-TTGACTGCTGTGGACTTG-3'; VEGF-reverse 5'-GCTGGGTTTGTCGGTGTT-3'; GAPDH-forward 5'-CAAGGTCATCCTGACAAC-3'; GAPDH-reverse 5'-GTCCACCACCCTGTTGCTGTAG-3'.

Quantification of VEGF expression by ELISA analyses

The human VEGF ELISA Kit (R&D, USA) was used to quantify the secreted VEGF in the cell supernatant, following the manufacturer's instructions.

Western blot analysis

Cells were washed three times with cold PBS and then lysed in RIPA buffer containing 50 mM Tris-HCl (pH 7.4), 1% NP-40, 0.25% sodium deoxycholate, 150 mM NaCl, 1 mM EDTA, 1 mM PMSF supplemented with 10% protease inhibitor cocktail (Sigma, USA), 1 mM sodium orthovanadate, and 1 mM sodium fluoride on ice for 30 min. Protein extracts were centrifuged at 12,000 g at 4°C for 10 min, and protein concentration was determined by micro bicinchonic acid assay (Thermo, USA) as directed by the manufacturer. Protein samples were subjected to 10% SDS-PAGE (50 g/lane) and then transferred onto PVDF membranes in Tris-glycine buffer containing 20% methanol. After blocking with PBS containing 5% bovine serum albumin for 2 h at room temperature, the membranes were incubated with anti-phospho-p38 antibody (1:1,000 dilution, Cell Signaling Technology, USA), anti-p38 antibody (1:1,000 dilution, Abgent, USA) or anti--Actin antibody (Sigma, USA) at 4°C overnight. After washes, membranes were then incubated with rabbit IgG HRP-linked secondary antibody (CST, USA) at 1:10,000 dilution for 1 h at room temperature, followed by a chemiluminescent reaction (Millipore, USA) and exposure to films. The intensity of the bands was quantified by densitometry (Wealtec, USA).

Statistical analysis

All experiments were repeated 3 times, and data were expressed as mean values plus or minus the standard error of the mean. An unpaired Student's *t* test was used for single comparisons. Statistical significance between experimental groups was determined using one-way ANOVA. *P*-value less than 0.05 was considered statistically significant. Data analysis was performed using SPSS 18.0 software.

Results

Characteristic of hASCs

hASCs were isolated from adipose tissue by collagenase digestion. The isolated cells exhibited a fibroblast-like morphology in primary culture. After a few days, hASCs expanded and the cells showed an elongated or oval/round shape with smooth borders (**Figure 1A**). To directly validate the multi-potency of the isolated cells,
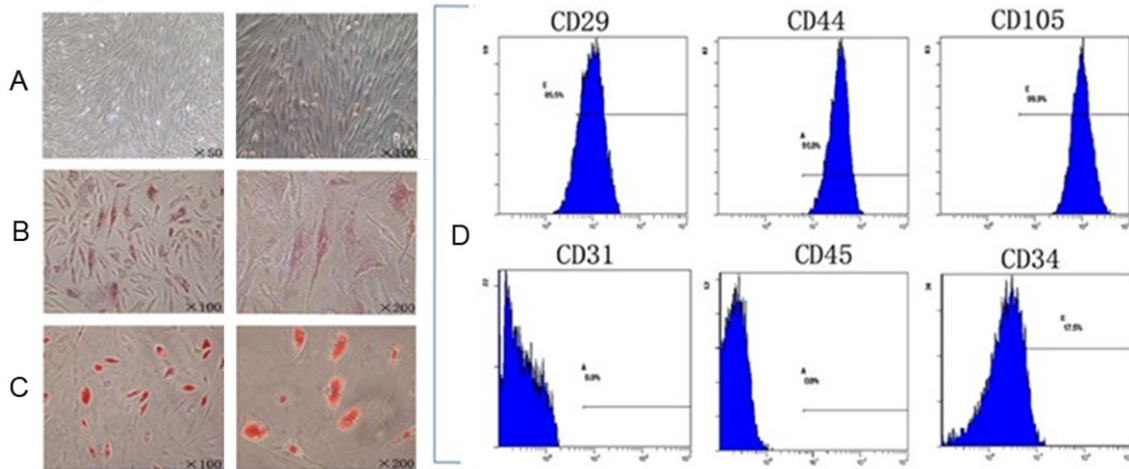
Figure 1. A. hASCs expanded and the cells showed an elongated or oval/round shape with smooth borders. B. Osteogenic differentiation by ALP staining. C. Adipogenic differentiation by Oil red O staining. D. Flow cytometry histograms of hASCs at passage 3 show the expression (shaded) of selected surface markers. CD29, 85.5%; CD45, 99.0%; CD105, 99.9%; CD31, 0.0%; CD45, 0.0%; CD34, 17.5%.
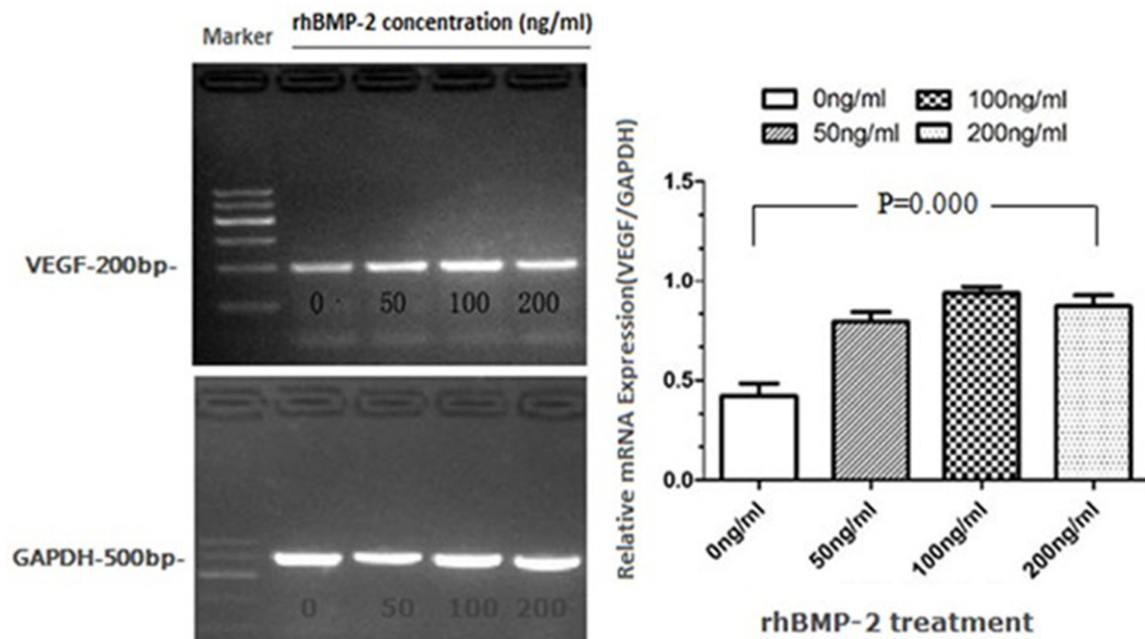
Figure 2. RT-PCR analysis of VEGF expression with different concentrations of rhBMP-2 treatments for 24 h. Total RNA was prepared and subjected to RT-PCR. GAPDH was used as a control. The intensities of the bands were analyzed by gel imaging and analysis system. *P* values were determined by unpaired Student's *t* test.

hASCs were cultured in osteogenic or adipogenic media for two weeks, and the differentiation into these lineages was confirmed by ALP staining and Oil red O, respectively (**Figure 1B** and **1C**), indicating that the isolated hASCs retain the multi-potency. More than 85% of the cells expressed CD29, and more than 99% expressed CD44 and CD105. In contrast, cells were negative for CD31 and CD45, and only 17.5% expressed CD34 (**Figure 1D**). This is consistent with the previous reports that human mesenchymal stem cells express CD29, CD44 and CD105 surface markers, while lack CD31, CD45 and CD34 expression, suggesting that the isolated hASCs possess the properties of mesenchymal stem cells.

Table 1. ELISA analysis of VEGF expression at different concentrations of rhBMP-2. F value is ratio of mean square (effect term/ error term). F value is associated with difference between interventions. *P* value is the result of comparison between groups

rhBMP-2	VEGF (ng/L)
0 ng/ml	1325.87±81.25
50 ng/ml	1384.70±199.01
100 ng/ml	1739.88±130.44
200 ng/ml	1541.85±143.13
F value	4.92
p value	0.03

rhBMP-2 induced VEGF expression inhASCs in a dose-dependent manner

To further characterize rhBMP-2-induced VEGF expression, hASCs were cultured in different concentrations of rhBMP-2for 24 h. The expression of VEGF was significantly elevated by RT-PCR analyses, with the highest induction observed at 100 ng/ml of rhBMP-2 (**Figure 2**). Consistently, the secreted VEGF protein in response to 100 ng/ml of rhBMP-2 treatment was significantly higher than the control group by ELISA analysis (**Table 1**). Interestingly, VEGF induction in response to 200 ng/ml of rhBMP-2 was lower than that of the 100 ng/ml dose, suggesting that 100 ng/ml of rhBMP-2 might be the most effective concentration to induce angiogenesis of hASCs.

rhBMP-2 stimulated VEGF expression inhASCs in a time-dependent manner

To further analyze the biological characteristics of rhBMP-2 effect on VEGF induction inhASCs, we studied the kinetics of VEGF expression in response to rhBMP-2. Since the 100 ng/ml of rhBMP-2 was shown to be most effective in inducing VEGF in these cells, the following experiments were fixed with this concentration. Interestingly, initial rhBMP-2 treatment between 3 h and 6 h resulted in a decrease in VEGF expression by RT-PCR (**Figure 3**). At 12 h, the expression of VEGF returned to the untreated level. The induction of VEGF was observed at 18 h and 24 h of treatments, while it returned to the basal levels at 36 h post rhBMP-2 challenge (**Figure 3**). A similar profile of secreted VEGF protein in response to rhBMP-2 was obtained with ELISA assays (**Table 2**). These results suggest that rhBMP-2 may have biphasic effect on VEGF expression, and it may suppress the initial VEGF levels, resulting in opposite biological functions.

The role of p38MAPK pathway in rhBMP-2 induced VEGF expression

To explore the regulatory mechanisms of rhBMP-2 induced VEGF expression, we investigated the phosphorylation of p38 (p-p38) at different concentrations and time points following rhBMP-2induction by Western blot analysis. The phosphorylation of p38 was observed with 50 ng/ml and 100 ng/ml of rhBMP-2 treatment (**Figure 4**). Further quantification revealed that the phosphorylated p38 in response to 50 ng/ml and 100 ng/ml of rhBMP-2 were 1.43× and 1.57× fold of that in the control group, respectively. Interestingly, 200 ng/ml of rhBMP-2 did not effectively induced p38 phosphorylation, consistent with the previous data that rhBMP-2 did not induce significant VEGF expression under this condition (**Figure 2** and **Table 1**).

To further analyze the role of p38MAPK pathway in rhBMP-2 induced VEGF expression, we studied the phosphorylation of p38 at various time points. The highest level of p38 phosphorylation was observed at 24 h post rhBMP-2 treatment (**Figure 5**), which correlated with the peak of VEGF expression (**Figure 3**). Interestingly, the level of p38 protein was also increased at 24 h time point with or without rhBMP-2 treatment (**Figure 5**). In contrast, p38 phosphorylation was decreased at 6 h post rhBMP-2 stimulation, consistent with the reduced VEGF expression at this time point (**Figure 3**). These results suggest a close correlation between p38 activation and VEGF induction.

Pretreatment with p38 inhibitor sb203580

To address whether the activation of p38 MAPK pathway is required for the stimulation of VEGF expression in hASCs, we blocked the p38 MAPK pathway using a specific inhibitor sb203580[26]. Pretreatment of hASCs with various doses of sb203580 significantly inhibited rhBMP-2 induced VEGF expression (**Figure 6**). VEGF levels were suppressed by 22.0% and 100% with sb203580 at concentrations of 5 M and 15 M, respectively. Consistently, ELISA
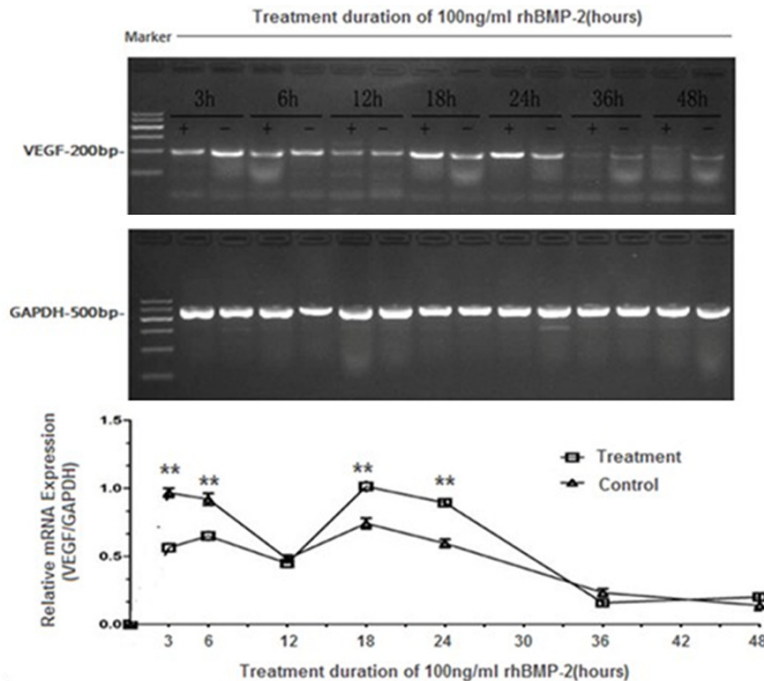
Figure 3. RT-PCR analyses of VEGF expression at different time points. hASCs were either left untreated or treated with 100 ng/ml of rhBMP-2 for indicated time points. Total RNA was prepared and subjected to RT-PCR. GAPDH was used as a control. The intensities of the bands were analyzed by gel imaging and analysis system. *P* values were determined by unpaired Student's *t* test (Treatment group vs Control group, *p < 0.05, **p < 0.01).

showed that the secreted VEGF levels were also suppressed by 15.0% and 100%, respectively, under these conditions (**Table 3**). These results suggest that the p38MAPK pathway is required for BMP-2-induced VEGF expression and angiogenesis.

Discussion

Recently, various methods have been explored to promote the angiogenesis of engineered bone tissue. One of these methods is to utilize growth factors. Among these growth factors, BMP-2 seems to hold the most promising prospect. BMP-2 has been widely utilized as a strong osteo-inducing factor for bone tissue repair and regeneration in both experimental studies and clinical applications. It has been shown that local BMP-2 application can rescue the delayed osteotomy healing in a rat model, and the mechanical stability of BMP-treated tibiae showed a significant increase as compared to that of the control group [28]. In clinic, BMP has been used in adult and pediatric spine surgeries with promising results [1, 16]. Our previous studies documented that rhBMP-2

could stimulate the expression of VEGF to enhance the angiogenesis of tissue engineered bone. It was also shown that the angiogenesis of human adipose-derived stromal cells (hASCs) was enhanced through knockdown of a BMP-2 Inhibitor [13]. Despite the positive effect of rhBMP-2 on vascularization, the detailed characteristics and the underlying mechanisms of BMP-2 mediated effect are not clear. A better understanding of BMP-2 effect can facilitate the development of effective strategies to promote the angiogenesis of engineered bone tissues utilizing rhBMP-2.

Our studies provided further characterization of rhBMP-2-stimulated VEGF expression in hASCs, and demonstrated that rhBMP-2 induces VEGF expression in a dose- and time-dependent manner. The optimal VEGF induction was observed at 24 h with 100 ng/ml of rhBMP-2 treatment, while a reduced VEGF induction was observed with a higher level of rhBMP-2 at 200 ng/ml (**Figure 2** and **Table 1**). It has been suggested that high doses of BMP-2 correlated with increased postoperative edema and swallowing complications after cervical fusion [6]. Our results support this notion, suggesting that high concentrations of rhBMP-2 may have adverse effect on the angiogenesis. In addition, rhBMP-2-induced VEGF expression appears to be biphasic. During 3-6 h, VEGF expression was reduced by BMP-2, while the induction of VEGF was observed at 18-24 h post BMP-2 stimulation. This observation may indicate that early application of rhBMP-2 to promote the angiogenesis of tissue engineered bone may not be beneficial, and 18-24 h might be the optimal time of utilizing rhBMP-2 to induce angiogenesis.

The p38 signaling pathway can profoundly modulate cell proliferation, differentiation, and

Table 2. ELISA analysis of VEGF expression at different time points of rhBMP-2 treatments. T value is the result of significant test to the mean of samples

Group	3 h	6 h	12 h	18 h	24 h	36 h	48 h
Treatment	1352.77±73.16	1384.70±99.01	1099.25±176.63	1735.69±105.00	1739.88±130.42	566.46±154.38	581.94±177.89
Control	1676.69±169.45	1606.55±140.67	1099.25±247.43	1484.70±66.86	1325.87±81.25	516.70±129.84	505.33±149.95
T value	-3.04	-1.58	0.00	3.49	4.67	0.43	0.57
p value	0.04	0.19	1.00	0.03	0.01	0.69	0.60
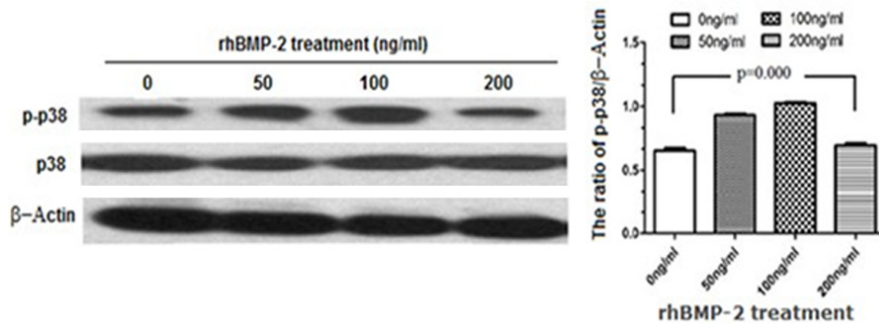
Figure 4. Western blot analysis of p38 activation in response to different concentrations of rhBMP-2 at 24 h post treatment. Whole protein extracts (50 μg/lane) were subjected to SDS-PAGE, followed by Western blot with an antibody specific for phosphorylated p38 (P-P38; top panel), an antibody recognizing total p38 (middle panel), or β-actin (bottom panel) as loading controls. The intensities of the bands were quantified by densitometry. P values were determined by unpaired Student's t test.

Figure 5. Western blot analysis of p38 activation at various time points in response to rhBMP-2 treatment at 100 ng/ml. Whole protein extracts (50 μg/lane) were subjected to SDS-PAGE, followed by Western blot with an antibody specific for phosphorylated p38 (P-P38; top panel), an antibody recognizing total p38 (middle panel), or β-actin (bottom panel) as loading controls. The intensities of the bands were quantified by densitometry. P values were determined by unpaired Student's t test.

between p38 phosphorylation and VEGF induction. Our data support the hypothesis that p38 MAPK pathway is involved in rhBMP-2 induced angiogenesis. Pretreatment of hASCs with the p38 inhibitor sb203580 abolished rhBMP-2 induced VEGF expression, further supports this hypothesis.

Conclusion

Our results indicate that rhBMP-2 stimulated VEGF expression of hASCs in a dose- and time-dependent manner. 100 ng/ml of rhBMP-2 might be the optimal dose of inducing angiogenesis, and 3-6 h and 18-24 h are two important time points. In addition, we revealed that rhBMP-2 could enhance the phosphorylation of p38 to promote VEGF expression. Information derived from this study may shed light on understanding the effect of rhBMP-2 in the angiogenesis of hASCs, which is important for designing new strategies to increase the angiogenesis of tissue engineering bone. The mech-

survival by influencing gene transcription in the nucleus in response to changes in the extracellular environment [12, 18]. Our results revealed that p38 is activated in response to BMP-2 in hASCs, and that there is a close correlation
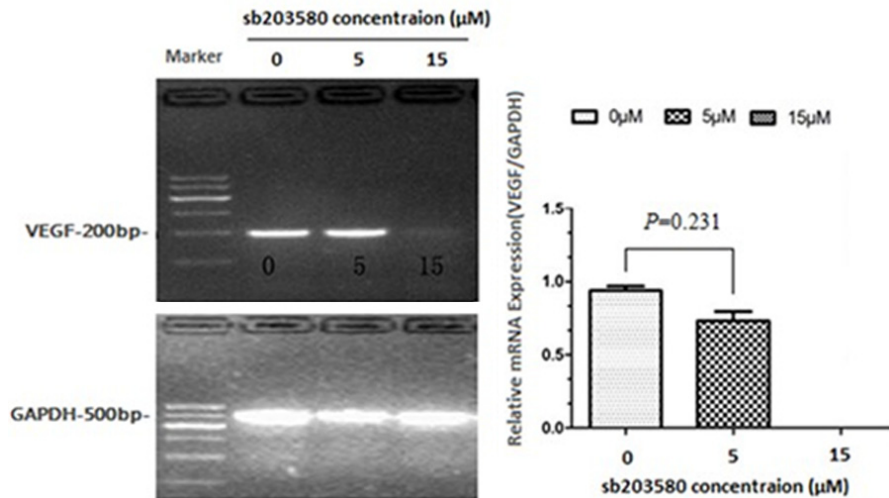
Figure 6. RT-PCR analyses of VEGF expression after pretreatments with a specific p38 pathway inhibitor, sb203580.hASCs were pretreated with sb203580 at indicated doses for 30 min, followed by 100 ng/ml of rhBMP-2 stimulation for 24 h. Total RNA was prepared and subjected to RT-PCR. GAPDH was used as a control. The intensities of the bands were analyzed by gel imaging and analysis system. P values were determined by unpaired Student's t test.

Table 3. ELISA analysis of VEGF expression with sb203580 pretreatment. F value is ratio of mean square (effect term/error term). F value is associated with difference between interventions. P value is the result of comparison between groups

sb203580 (μM)	VEGF (ng/L)
0	1706.55±183.45
5	1449.98±123.00
15	0.00±0.00
F value	156.22
P value	0.00

anism of rhBMP-2-mediated inhibition of VEGF expression at early time points (3-6 h) needs to be further explored.

Acknowledgements

Disclosure of conflict of interest

None.

Address correspondence to: Dr. Jiang Wu, School of West China Basic Medicine and Forensic Medicine, Sichuan University; Lab. of Cardiovascular Disease, West China Hospital of Sichuan University, Chengdu 610041, P.R. China. Tel: +86 18699133980; E-mail: jw@scu.edu.cn

References

[1] Carlisle E, Fischgrund JS. Bone morphogenetic proteins for spinal fusion. Spine J 2005; 5: 240-S-249S.

[2] Cui L, Yin S, Liu W, Li N, Zhang W, Cao Y. Expanded adipose-derived stem cells suppress mixed lymphocyte reaction by secretion of prostaglandin E2. Tissue Eng 2007; 13: 1185-1195.

[3] des Rieux A, Ucakar B, Mupendwa BP, Colau D, Feron O, Carmeliet P, Preat V. 3D systems delivering VEGF to promote angiogenesis for tissue engineering. J Control Release 2011; 150: 272-278.

[4] Drosse I, Volkmer E, Capanna R, De Biase P, Mutschler W, Schieker M. Tissue engineering for bone defect healing: an update on a multicomponent approach. Injury 2008; 39 Suppl 2: S9-20.

[5] Esther CN, Claudia K, Petra JK. Vascularization is the key challenge in tissue engineering. Advanced Drug Delivery Reviews 2011; 63: 300-311.

[6] Fred N, Lee W, Moshe L, Claudio P. BMP-2 dose correlates with increased postoperative edema and swallowing complications after cervical fusion. Spine Journal 2006; 6: 7S-8S

[7] Gamell C, Osses N, Bartrons R, Ruckle T, Camps M, Rosa JL, Ventura F. BMP2 induction of actin cytoskeleton reorganization and cell migration requires PI3-kinase and Cdc42 activity. J Cell Sci 2008; 121: 3960-3970.

[8] Gazdag AR, Lane JM, GlaserD, Forster RA. Alternatives to Autogenous Bone Graft: Efficacy and Indications. J Am Acad Orthop Surg 1995; 3: 1-8.

[9]   Gee E, Milkiewicz M, Haas TL. p38 MAPK activity is stimulated by vascular endothelial growth factor receptor 2 activation and is essential for shear stress-induced angiogenesis. J Cell Physiol 2010; 222: 120-126.

[10]   Greenblatt MB, Shim JH, Zou W, Sitara D. The p38 MAPK pathway is essential for skeletogenesis and bone homeostasis in mice. J Clin Invest 2010; 120: 2457-2473.

[11]   Junttila MR, Li SP, Westermarck J. Phosphatase-mediated crosstalk between MAPK signaling pathways in the regulation of cell survival. FASEB J 2008; 22: 954-965.

[12]   Kim J, Wong PK. Loss of ATM impairs proliferation of neural stem cells through oxidative stress–mediated p38 MAPK signaling. Stem Cells 2009; 27: 1987-1998.

[13]   Levi B, Nelson ER, Hyun JS, Glotzbach JP, Li S, Nauta A, Montoro DT, Lee M, Commons GC, Hu S, Wu JC, Gurtner GC, Longaker MT. Enhancement of human adipose-derived stromal cell angiogenesis through knockdown of a BMP-2 inhibitor. Plast Reconstr Surg 2012; 129: 53-66.

[14]   Liu Q, Cen L, Zhou H, Yin S, Liu G, Liu W, Cao Y, Cui L. The role of the extracellular signal-related kinase signaling pathway in osteogenic differentiation of human adipose-derived stem cells and in adipogenic transition initiated by dexamethasone. Tissue Eng Part A 2009; 15: 3487-3497.

[15]   Logeart-Avramoglou D, Anagnostou F, Bizios R, Petite H. Engineering bone: challenges and obstacles. J Cell Mol Med 2005; 9: 72-84.

[16]   Mladenov KV, Kunkel P, Stuecker R. The use of recombinant human BMP-2 as a salvage procedure in the pediatric spine: a report on 3 cases. Eur Spine J 2010; 19 Suppl 2: S135-139.

[17]   Nkenke E, Weisbach V, Winckler E, Kessler P, Schultze-Mosgau S, Wiltfang J, Neukam FW. Morbidity of harvesting of bone grafts from the iliac crest for preprosthetic augmentation procedures: a prospective study. Int J Oral Maxillofac Surg 2004; 33: 157-163.

[18]   Oeztuerk-Winder F, Ventura JJ. The many faces of p38 mitogen-activated protein kinase in progenitor/stem cell differentiation. Biochem J 2012; 445: 1-10.

[19]   Porter JR, Ruckh TT, Popat KC. Bone tissue engineering: a review in bone biomimetics and drug delivery strategies. Biotechnol Prog 2009; 25: 1539-1560.

[20]   Sandra D, Mathias K, Anna EP, Sabine N, Ziyang Z, Ursula H, Ann KR, Caroline W, Thilo, LS, Tim B, Charli K, Hans-Günther M, José TE. The use of human sweat gland-derived stem cells for enhancing vascularization during dermal regeneration. Journal Investigative Dermatology 2012; 132: 1707-1716.

[21]   Seebach C, Henrich D, Kahling C, Wilhelm K, Tami AE, Alini M, Marzi I. Endothelial progenitor cells and mesenchymal stem cells seeded onto beta-TCP granules enhance early vascularization and bone healing in a critical-sized bone defect in rats. Tissue Eng Part A 2010; 16: 1961-1970.

[22]   Shields LB, Raque GH, Glassman SD, Campbell M, Vitaz T, Harpring J, Shields CB. Adverse effects associated with high-dose recombinant human bone morphogenetic protein-2 use in anterior cervical spine fusion. Spine (Phila Pa 1976) 2006; 31: 542-547.

[23]   Song I, Kim BS, Kim CS, Im GI. Effects of BMP-2 and vitamin D3 on the osteogenic differentiation of adipose stem cells. Biochem Biophys Res Commun 2011; 408: 126-131.

[24]   Tang CL, Mahoney JL, McKee MD, Richards RR, Waddell JP, Louie B. Donor site morbidity following vascularized fibular grafting. Microsurgery 1998; 18: 383-386.

[25]   Wang Q, Huang C, Xue M, Zhang X. Expression of endogenous BMP-2 in periosteal progenitor cells is essential for bone healing. Bone 2011; 48: 524-532.

[26]   Wang X, Cui L, Joseph J, Jiang B, Pimental D, Handy DE, Liao R, Loscalzo J. Homocysteine induces cardiomyocyte dysfunction and apoptosis through p38 MAPK-mediated increase in oxidant stress. J Mol Cell Cardiol 2012; 52: 753-760.

[27]   Watanabe-Takano H, Takano K, Keduka E, Endo T. M-Ras is activated by bone morphogenetic protein-2 and participates in osteoblastic determination, differentiation, and transdifferentiation. Exp Cell Res 2010; 316: 477-490.

[28]   Wildemann B, Lange K, Strobel C, Fassbender M. Local BMP-2 application can rescue the delayed osteotomy healing in a rat model. Injury 2011; 42: 746-52.

[29]   Zou D, Zhang Z, He J, Zhang K, Ye D, Han W, Zhou J, Wang Y, Li Q, Liu X, Zhang X, Wang S, Hu J, Zhu C, Zhang W, zhou Y, Fu H, Huang Y, Jiang X. Blood vessel formation in the tissue-engineered bone with the constitutively active form of HIF-1alpha mediated BMSCs. Biomaterials 2012; 33: 2097-2108.

[30]   Zuk PA, Zhu M, Ashjian P, De Ugarte DA, Huang JI, Mizuno H, Alfonso ZC, Fraser JK, Benhaim P, Hedrick MH. Human adipose tissue is a source of multipotent stem cells. Mol Biol Cell 2002; 13: 4279-4295.